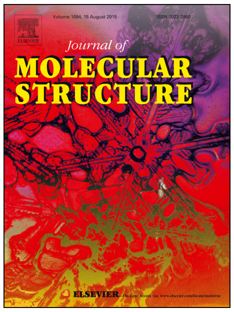

Experimental and quantum chemical studies of a new organic proton transfer compound, 1H-imidazol-3-ium-3-hydroxy-2,4,6-trinitrophenolate

P. Dhamodharan, K. Sathya, M. Dhandapani

PII: S0022-2860(17)31355-8

DOI: 10.1016/j.molstruc.2017.10.024

Reference: MOLSTR 24395

To appear in: *Journal of Molecular Structure*

Received Date: 6 July 2017

Revised Date: 5 October 2017

Accepted Date: 6 October 2017

Please cite this article as: P. Dhamodharan, K. Sathya, M. Dhandapani, Experimental and quantum chemical studies of a new organic proton transfer compound, 1H-imidazol-3-ium-3-hydroxy-2,4,6-trinitrophenolate, *Journal of Molecular Structure* (2017), doi: 10.1016/j.molstruc.2017.10.024.

Graphical Abstract

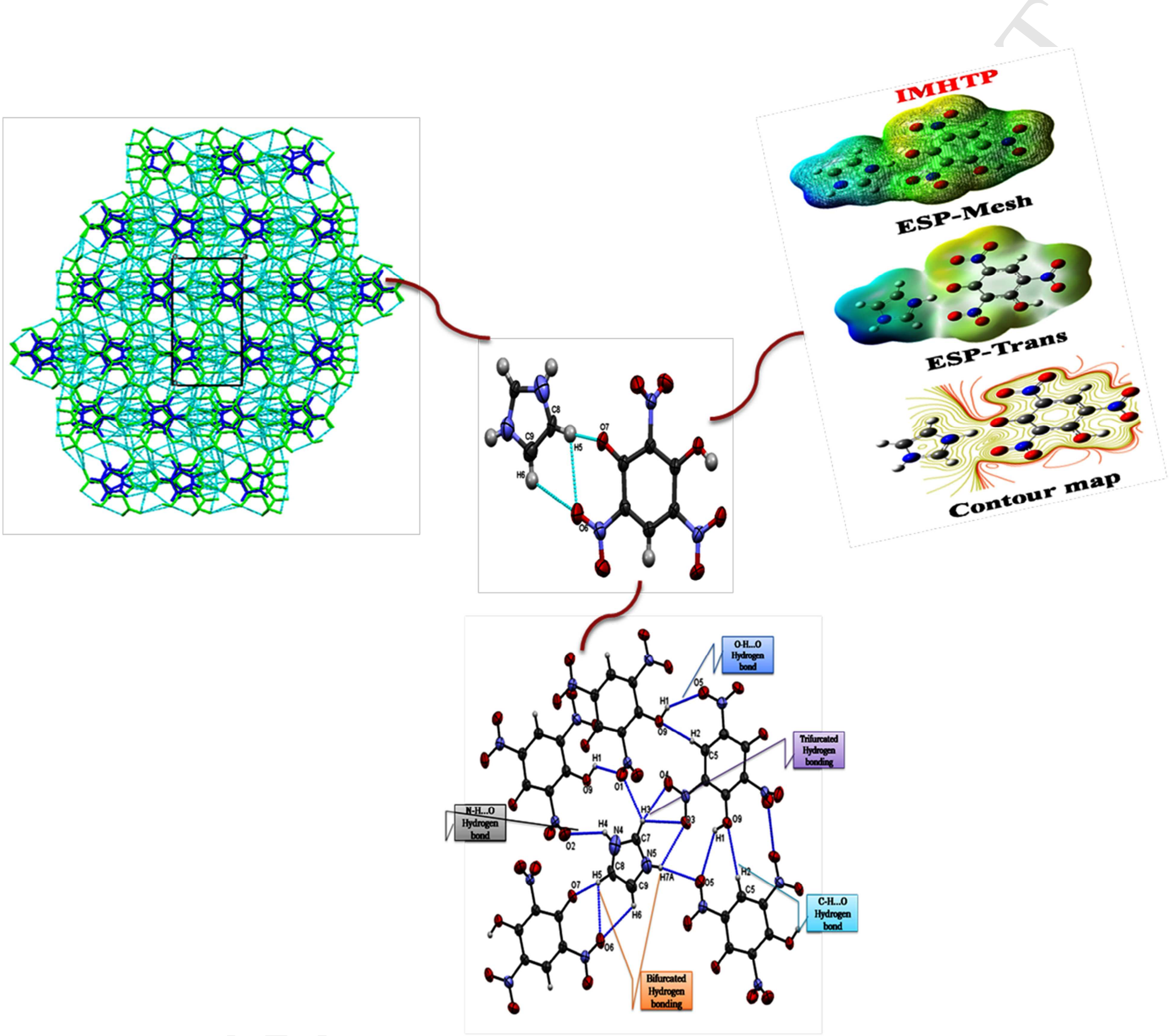

Experimental and quantum chemical studies of a new organic proton transfer compound, 1H-imidazol-3-ium-3-hydroxy-2,4,6-trinitrophenolate

P. Dhamodharan, K. Sathya and M. Dhandapani *

Department of Chemistry, Sri Ramakrishna Mission Vidyalaya College of Arts and Science, Coimbatore-641 020, Tamil Nadu, India.

*Corresponding Author’s E-mail: srmvdhandapani@gmail.com; Phone: +91 94420 01232.

Keywords:

Proton transfer, Hydrogen bonding, Hyperpolarizability, Optical materials.

Abstract

A new proton transfer compound, 1H-imidazol-3-ium-3-hydroxy-2, 4, 6 trinitrophenolate (IMHTP), was crystallized by slow evaporation-solution growth technique. ^{1}H and ^{13}C NMR spectral studies confirm the molecular structure of the grown crystal. Single crystal X-ray diffraction study confirms that IMHTP crystallizes in monoclinic system with space group P_{21}/c. Thermal curves (TG/DTA) show that the material is thermally stable up to 198 °C. The crystal emits fluorescence at 510 nm, proving its utility in making green light emitting materials in optical applications. The stable molecular structure was optimized by Gaussian 09 program with B3LYP6-311++g(d,p) level of basis set. The frontier molecular orbital study shows that the charge transfer interaction occurs within the complex. The calculated first order hyperpolarizability value of IMHTP is 44 times higher than that the reference material, urea. The electrostatic potential map was used to probe into electrophilic and nucleophilic reactive sites present in the molecule.

1. Introduction

Organic materials are attractive due to their electronic and optical properties. The molecular structure of organic molecules can be easily designed and modified for suitable applications [1]. The growth of organic crystals has gained much importance for the fabrication of technologically important devices in electronics and optical applications [2-5]. Organic molecules are composed of skeletons with hetero atoms such as N, O and S etc other than carbon hydrogen atoms. The fact behind their use in optical applications is due to the generation of hydrogen bonding net work in the crystalline state.

Hydrogen bonding plays a vital role in chemical, catalytic and biochemical processes, chemical engineering, as well as in supramolecular chemistry [6-9]. Hydrogen bonding is the widely used non-covalent interaction in many organic materials due to their aggregation into self-assembly. The design and construction of multi-component supramolecular synthons utilizing hydrogen bonding is one of the rapidly developing areas in supramolecular synthesis [10-12]. Organic Lewis acid - Lewis base combinations have gained popularity in recent years because they have the potential to alter and optimize physical properties such as crystalline form, solubility and stability [13-17]. Heterocyclic compounds containing nitrogen atom in particular are useful in the construction of optically important crystals. Imidazole is an organic heterocyclic nitrogenous compound containing two electron rich nitrogen atoms. These electronegative nitrogen atoms can be centers of hydrogen bonding networks which can stabilize the crystal system. The alternate nitrogen atoms in imidazole can involve in charge transfer activity for improving optical property when coupled with suitable acidic components. Imidazole can act a Lewis base and form a stable complex with styphnic acid. We have already reported the synthesis and application of a few organic crystals in the combination of styphnic acid and heterocyclic bases [18-24].

In this present work, we report structural, experimental, quantum chemical analysis and thermal investigations of a new organic molecular crystal, 1H-imidazol-3-ium-3-hydroxy-2,4,6-trinitrophenolate involving proton transfer mechanism.

2. Experimental section

2.1 Synthesis of 1H-imidazol-3-ium-3-hydroxy-2,4,6-trinitrophenolate (IMHTP)

Commercially available 1H-imidazole (sigma Aldrich-analytical grade) and laboratory synthesized styphnic acid were taken as the starting materials for the synthesis of IMHTP. The styphnic acid and 1H-imidazole were dissolved separately in equimolar ratio in pure methanol and mixed thoroughly together. The resulting solution was stirred well for 10 minutes to get a yellow colour precipitate. The suspended impurities were removed through a Whatmann 41 grade filter paper. Bright yellow coloured crystals were harvested after ten days from the saturated solution in acetone. The purity of the crystal was improved by repeated recrystallizations. The reaction scheme for the synthesis is represented below,

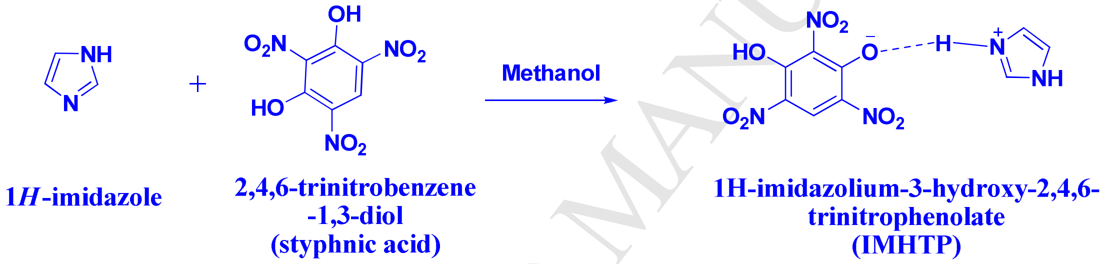

2.2 Physico-chemical characterization of IMHTP

Elemental analysis was performed in a flash EA 1112 fully automatic trace element analyzer. Molecular weight of $C_9H_7N_5O_8$ is 313.20. The experimental and calculated values in percentage are: Found: C, 34.65; H, 2.21; N, 22.26, Calculated for C, 34.52; H, 2.25; N, 22.36. The experimental and calculated values are in good agreement with each other and this observation indicates that the IMHTP is free from impurities. The FT-IR spectrum (Fig. 1) of IMHTP was recorded in the region 4000-400 cm^{-1} using a JASCO FT/IR 5300 infrared spectrometer. The FT-IR wave numbers (cm^{-1}) of selected bands are: υ=3305 (O-H), 3083 (N-H), 1592 $(NO_2)_{asy}$, 1377 $(NO_2)_{sy}$, 1445 (C=C), 849 (C-H), 1620 (C=N), 1299 (C-N), 1269 (C-O). The FT-Raman wave numbers (cm^{-1}) are : υ=1579 $(NO_2)_{asy}$, 1318 $(NO_2)_{sy}$, 1450 (C=C), 827 (C-H), 1624 (C=N), 1334 (C-N), 1296 (C-O). ^{1}H and ^{13}C NMR spectroscopic data were recorded on a Bruker Avance 400 MHz FT-NMR instrument with tetramethylsilane (TMS) as an internal standard using DMSO-d_6 solvent. ^{1}H NMR chemical shifts δ (in ppm) of various protons are:

13.1 (s, OH, NH), 8.6 (s, for both H5 & H6), 9.1 (s, H3), 7.7 (s, H2). The chemical shifts (δ ppm) in ^{13}C NMR are: 156.2 (C1 and C3), 126.1 (C5), 135.8 (C2, C4 and C6), 134.8 (C7), 119.7 (C8 and C9). It is observed that the signal for OH and NH protons submerge and appear as a broad hump in the deshielded region in ^{1}H NMR spectrum [24]. The ^{1}H and ^{13}C NMR spectra and theoretical values are given in Fig. 2 and Table 1 respectively.

3. Results and discussion

3.1 Structural determination of IMHTP

The crystallographic data of IMHTP have been collected at 298 K on a Bruker SMART APEX CCD with area detector system (MoKα = 0.7103 Å). Data reduction, absorption correction and refinements were carried out by SAINT PLUS, SADABS and SHELXL-97 software, respectively [33-34]. Non-hydrogen atoms were refined with anisotropic thermal parameters.

The ORTEP diagram of IMHTP is shown in Fig. 3a. The compound IMHTP crystallizes in monoclinic system with space group $P2_1/c$. The lattice parameters are a = 6.0000(12) Å, b = 13.100(3) Å, c = 15.000(3) Å, α =90°, β = 94.00 (3)° and γ= 90°. The unit cell volume (V) is= 1176.1(4) Å^3 and the number of molecules in unit cell (Z) is 4. The total no of reflections collected are 6459. The crystallographic parameters IMHTP are shown in the Table 3. The bond lengths of C1-C2 and C1-C6 are 1.429 and 1.443 Å, respectively which are longer than the standard aromatic (C-C single bond length (1.40 Å) value. The bond length of C1-O7 in IMHTP is 1.235 Å which is shorter than that of normal bond length C-O (1.339 Å). The C1-O7 value is intermediate between the single and double bonds. It is clear that a proton migrates from one of the hydroxyl groups of styphnic acid to the hetero nitrogen atom of imidazole during the reaction. The loss of hydroxyl proton at the O7 leads to specific electron delocalization around C1 atom.

The electron withdrawing nitro group, decreases the electron density of the C atom linked to it leading an increase in the bond angles of C(1)-C(2)-C(3) and C(1)-C(6)-C(5) with values 126.9 and 122.9°, respectively. The asymmetric unit consists of one imidazolium cation and one styphnate anion. All the three nitro groups possess planar geometry. It is interesting note that only one of the nitro group plane deviates greatly from the normal benzene ring at an angle 67.95° (O2-N1-O1). The other two nitro groups are slightly off-plane with respect to aromatic benzene ring in styphnate moiety. The deviation angles of O3-N2-O4 and O5-N3-O6 are 1.94 and 6.10°, respectively. Due to the large deviation in (O2-N1-O1) nitro group, the styphnate anion undergoes different kinds of covalent and non-covalent interactions like hydrogen bond, van der Waals interactions including bifurcated and trifurcated arrangements. The styphnic acid-Lewis base combinations are stabilized through numerous hydrogen bonding interactions in the crystal lattice. Packing view diagram of IMHTP is shown in Fig. 4.

Hydrogen bonding network between the donor and acceptor moieties of IMHTP is shown in Fig. 4. Supramolecules composed of strong N-H…O and O-H…O hydrogen bonds and weak C-H…O bonds are known to play a considerable role in determining the packing of organic crystals [37]. The hydrogen atom (H3) present in C7 is involved in a trifurcated hydrogen bond with nitro oxygen atoms of styphnic acid through weak C-H…O (C7-H3…O1/O3/O4) interactions. The other hydrogen atom (H5) of imidazole forms bifurcated hydrogen bonding with neighbouring deprotonated oxygen atom (O7) and nitro oxygen (O6) of styphnic acid (C8-H5…O7/O6).

Furthermore, the cationic imidazole moiety makes hydrogen bond with neighbouring anionic moiety of styphnic acid. The imidazole hydrogen atom (H7A) forms bifurcated hydrogen bonding with two oxygen atoms of neighbouring styphnate (N5-H7A…O3/O5). Another strong N-H…O interaction is observed between hydrogen atom (H4) of imidazole and nitro oxygen atom (O2) of styphnate anion. In the imidazole cation, all the hydrogens involve in hydrogen bonding with neighbouring anionic moiety. The hydrogen atom (H6) of imidazole cation forms hydrogen bonding with neighbouring oxygen atom of styphnate anion through weak C9-H6…O6 interactions. Apart from these interactions, the C-H…O interaction is also observed between the two styphnate anions through C5-H2…O9 interactions.

3.2 Optical studies

It is a common requirement for any material to be used in optical applications that the crystal should possess a wide transparency in visible region and the lowest possible cut off wavelength [26]. The recorded UV-Vis absorption spectrum is shown in Fig. S1. The complex shows absorptions at 216, 332 and 401 nm. The absorptions at 216 and 332 nm are due to the n–π* transitions of the complex. The absorption at 401 nm is due to the π-π* transition. The n–π* and π-π* transitions of the complex are responsible for charge transfer and aromatic conjugation. The yellow colour of the crystal is due to the presence of chromophore, nitro (NO_2) and auxochromes hydroxyl group (-OH group) in styphnic acid. The transition is due to promotion of an electron from the higher energy state of the donor (imidazole) to the lower energy state of the acceptor (styphnic acid). The UV-Vis and UV-Vis-NIR spectra of IMHTP are shown in Fig. 2b. The IMHTP crystal is transparent from visible to NIR region an with optical cut-off at 400 nm. The absence of absorption between 470 and 900 nm shows that the crystal is transparent in this region attesting its suitability in frequency doubling applications.

3.3 Emission spectral analysis

Photoluminescence studies are useful in understanding the various types of energy transition states in a molecule [27-30]. The photoluminescence spectrum of IMHTP crystal was recorded in a Horiba Jobin-Yvon-FL3-22 Flurolog spectroflurometer. Fluorescence is expected generally in molecules that are aromatic or contain conjugated double bonds with a high degree of resonance stability [31]. The fluorescence emission spectrum of IMHTP crystal is shown in Fig. S2. The emission spectrum of the compound was measured in the wavelength range between 400 and 620 nm. The compound shows peak at 500 nm (λ_{ex}= 440 nm) in the emission spectrum. The broad peak at 500 nm indicates that IMHTP has a green fluorescence emission property revealing the use of the material in solid state lighting and display applications [32].

3.4 Thermal analysis

Thermal analysis was carried out to study the thermal stability and melting point of the grown crystal. Thermal analyses (TG/DTA) were performed by a Mettler Toledo Star SW 8.10 TG/DTA thermal analyzer between 30 and 500 °C under nitrogen atmosphere at a heating rate of 20 °C per minute. The TG/DTA thermogram of the crystal is shown in Fig. S3. From the TG curve, it is observed that there was no loss of weight around 100 °C. This confirms the absence of water in any form in the sample. A sharp exothermic peak at 198 °C clearly indicates the complete decomposition of the crystal. The mass of the IMHTP remains unchanged till 198 °C and the sample loses its weight almost completely around 230 °C. TG curve shows a single stage weight loss which is due to complete degradation of the crystal into fragments and its subsequent volatilization into various gaseous fractions like CO, CO_2, NO_2 and, NH_3. Absence of either endothermic or exothermic peaks below 198 °C indicates that there was no phase transition before the melting point. The sharpness of the exothermic peak infers good degree of crystallinity of the grown crystal. Therefore, IMHTP crystal is suitable for optical applications up to 198 °C.

3.5 Optimized geometry

The optimized molecular structure of IMHTP was calculated using B3LYP-6-311++ G(d,p) basis set and is shown in Fig. 3b. The structural parameters obtained from the DFT method are presented in Table 2. Theoretically optimized bond lengths and angles are larger than the experimental ones since the theoretical calculation were done assuming isolated molecule in gaseous phase.

3.6 Frontier molecular orbital analysis

The FMO analysis furnishes a platform for understanding the phenomenon of charge transfer through optical molecular excitations [35,36]. The chemical hardness and reactivity of an optical material can be predicted from HOMO-LUMO energy gap. The calculated energies of HOMO and LUMO of IMHTP are -6.82eV and -3.15eV, respectively and the energy gap is found to be 3.66 eV. The ionization energy (I) and electron affinity (A) can be expressed through HOMO and LUMO orbital energies as $I = -E_{HOMO} = 6.824$ eV and $A = -E_{LUMO} = 3.156$ eV. The global hardness (η) is predicted by the relation $\eta = (I-A)/2 = 1.834$ eV. The electron affinity can be used in combination with ionization energy to give electronic chemical potential $\mu = -(E_{HOMO} + E_{LUMO})/2 = 4.95$ eV. The global electrophilicity index (ω) is given by $\omega = \mu^2/2\eta = 6.69$ eV.

The HOMO-LUMO plots of IMHTP are shown in Fig. 5 along with reactants molecules, imidazole and styphnic acid. In IMHTP, the HOMO electrons are localized on aromatic ring of styphnate anionic moiety (electron acceptor) and LUMO electrons are localized over upper part of the aromatic ring and two nitro groups leaving the third one free. Thus, the HOMO-LUMO transition implies an electron density transfer within the styphnate moiety through conjugated path. The HOMO-LUMO energy gap of styphnic acid, imidazole and IMHTP are 4.19, 6.05 and

3.66 eV, respectively. The energy gap in IMHTP is smaller than the reactant molecules which is a clear evidence for the stability of the product formed. The smaller gap facilitates strong hydrogen bonding in IMHTP which leads to the larger values of first order hyperpolarizability [37].

3.7 Molecular electrostatic potential map

In order to predict the nature of reactive sites in IMHTP, molecular electrostatic potential (MEP) analysis was undertaken. [38]. The MEP map for IMHTP crystal is shown in Fig. 6. The yellow, blue and green colour indicated as negative, positive and zero electrostatic potential. The negative region (yellow colour) of the MEP surface covers the styphnate moiety that represents the electrophilic reactivity sites and positive region (blue colour) spread over imidazole cation that indicates the nucleophilic reactivity sites. In the reactant molecules, the positive potential is spread over the N-H group of imidazole and benzene ring of styphnic cid while the negative potential localized over the nitro groups of styphnic acid and nitrogen atom of the imidazole molecule. The contour maps and MEP of the reactants, the product confirms the proton transfer from the proton donor to the acceptor. The MEP of IMHTP confirms the presence of various types of inter and intramolecular hydrogen bonding interactions [39].

3.8 Mulliken atomic charges

The electronic charge on the individual atoms in a molecule decides the bonding pattern. The atomic charge values were obtained by the Mulliken population analysis [40]. The structure of IMHTP with Mulliken atomic charges are shown in Fig. 7. The calculated results show that all the oxygen atoms of the styphnate and nitrogen atoms of the imidazolium are encompassed by negative charges. The positive charge is located over the carbon and hydrogen atoms of IMHTP molecule. Larger magnitude of negative charge is observed for nitrogen atoms of imidazole (N25 = -0.6809 e and N27 = -0.6407 e) and deprotonated oxygen atom (O29 = -0.5501 e) of the styphnate moiety. It is also observed that the nitrogen atoms of nitro group of styphnate moiety have smaller positive charges due to the delocalization of π electrons. The highest positive charge is identified in hydrogen atom (H2) (0.4042 e) of the unprotonated hydroxyl group of styphnate. Lesser positive charges are also found in the C7 (0.4091 e) and N27 (0.4348 e) atoms.

3.9 First order hyperpolarizability

During theoretical evaluation of a compound for nonlinear optical activity, calculation of first hyperpolarizability values are important. In this context, the dynamic first hyperpolarizability (β) of the title compound has been calculated using DFT method at the B3LYP/6-311++G (d,p) level of basis set. It is well known that the higher values of dipole moment, molecular polarizability and first order hyperpolarizability are important for more active NLO properties. A substantial delocalization of charges in a particular direction would bring about high value of hyperpolarizability in that direction. In IMHTP the highest value is found in β_{xxx} direction. The maximum β value may be due to π-electron cloud movement from donor to acceptor which makes the molecule highly polarized with possible intramolecular charge transfer.

The calculated total first-order polarizability (β) and the dipole moment (μ) values of IMHTP are 5.724×10^{-30} esu and 15.475 debye, respectively. The β value is approximately 44 times greater than that of urea. The hyperpolarizability value of IMHTP molecule plays an important role not only in the building up of the molecular structure but also in the enhancement of optical properties. The high β value is consequence of numerous intra and inter-molecular hydrogen bonds IMHTP. This great magnitude of the first hyperpolarizability suggests IMHTP can be used in the development of NLO materials. A comparison of first order hyperpolarizability for the constituents of IMHTP is listed in the Table 4.

3.10 Hirshfeld surface analysis

Hirshfeld surface analysis allows a quick and easy identification of the significant intermolecular interactions (C-H…π, O-H…O, H…H etc.) map on the molecular surface. CrystalExplorer, a computer program was used for calculation of Hirshfeld surfaces and 2D fingerprint plots [41]. The two-dimensional (2D) fingerprint plots obtained from Hirshfeld analysis provides a good amount of information on pattern of packing and atom-atom contacts. Fig. 8 represents 2D fingerprint plots and its percentage contributions of IMHTP crystal. The larger circular depressions (deep red) visible on the side of the 3D Hirshfeld surfaces correspond to the significant hydrogen bonding contacts. While the red color points indicate the short contacts of H...H, N…H and H...O interactions. The proportion of O…H/H…O interactions covers 52% of the total Hirshfeld surfaces with two distinct spikes in the 2D fingerprint plots indicating hydrogen bonding interactions are the most significant interactions in the crystal. The H…H interactions, which are reflected in the middle of scattered points in the 2D fingerprint plot comprise 7.8% of the total Hirshfeld surfaces. The presence of nitro and hydroxy groups is responsible for O…O (13.3%) and N…O/O…N (4.2 %), interactions in IMHTP. The O…C/C…O (5.6 %) and C…C (4.6 %) interactions are also observed in IMHTP. Hirshfeld surface analysis of IMHTP crystal demonstrated that O…H/H…O interaction is more prominent.

Conclusion

A new proton transfer crystal, 1H-imidazol-3-ium-3-hydroxy-2,4,6 trinitrophenolate (IMHTP) was synthesized by slow evaporation-solution growth method. The FT-IR and NMR spectroscopic analysis confirm the formation of the IMHTP. The compound has a green emission property so that it can be used for solid state lighting and display applications. The IMHTP crystallizes in monoclinic system with space group $P2_1/c$. The asymmetric unit consists of one imidazolium cation and one styphnate anion. The stability of crystal structure is governed by the numerous bifurcated and trifurcated strong N-H…O and O-H…O hydrogen bonds and weak C-H…O bonds networks. The IMHTP is thermally stable up to 198 °C. The optimized stable molecular structure of IMHTP was calculated using B3LYP-6-311++ G(d,p) basis set. The HOMO –LUMO energy gap is smaller (3.66 eV) in the product IMHTP, than the reactant molecules indicating the stability of the product. The contour maps of the reactants and MEP illustrates the proton transfer from the proton donor to the acceptor. Mulliken charge analysis indicates that the highest positive charge is found in hydrogen atom (0.4942 e) of the free hydroxyl group of styphnate while the highest negative is present in the carbon atom (0.4091e) having O^- atom. The calculated total first-order polarizability (β) and the dipole moment (μ) values are 5.724×10^{-30} esu and 15.475 debye respectively. The β value is approximately 44 times greater than that of the standard reference material, urea. The large transmittance, lower cut off wavelength, excessive hydrogen bonding, lowest band gap and high β value indicate that IMHTP material is an excellent candidate for optoelectronic applications.

Acknowledgements

One of the authors, M. Dhandapani, would like to thank the University Grants Commission (UGC), New Delhi, India for the financial support (Major Research Project Grant No. 43-200/2014(SR) to carry out the research work. P. Dhamodharan, thanks the Dr. R. Nagarajan, School of Chemistry and UGC Networking Centre, Hyderabad, for awarding visiting research fellowship.

References

[1] P.N. Prasad, D.J. Williams, Introduction to Nonlinear Optical Effects in Molecules and Polymers, Wiley, New York, 1990.

[2] A. Schneider, M. Neis, M. Stillhart, B. Ruiz, R. Khan, P. Gunter, Generation of terahertz pulses through optical rectification in organic DAST crystals: theory and experiment, J. Opt. Soc. Am. B **23** (2006) 1822.

[3] Y. Takahashi, H. Adachi, T. Taniuchi, M. Takagi, Y. Hosokawa, S. Onzuka, S. Brahadeeswaran, M. Yoshimura, Y. Mori, H. Masuhara, T. Sasaki, H. Nakanishi, Organic nonlinear optical DAST crystals for electro-optic measurement and terahertz wave generation, J.Photochem. Photobiol. A: Chem. **183** (2006) 247-252.

[4] L. Boubekeur-Lecaque, B.J. Coe, K. Clays, S. Foerier, T. Verbiest, I. Asselberghs, Redox-Switching of Nonlinear Optical Behavior in Langmuir−Blodgett Thin Films Containing a Ruthenium(II) Ammine Complex, J. Am. Chem. Soc. **130** (2008) 3286-3287.

[5] S. Bidault, J. Gouya, S. Brasselet, J. Zyss, Encoding multipolar polarization patterns by optical poling in polymers: towards nonlinear optical memories, Opt. Express **13** (2005) 505.

[6] C.B. Aakeröy, A.M. Beatty, B.A. Helfrich, “Total Synthesis” Supramolecular Style: Design and Hydrogen-Bond-Directed Assembly of Ternary Supermolecules, Angew. Chem. Int. Ed. **40** (2001) 3240-3242.

[7] T.R. Shattock, P. Vishweshwar, Z.Q. Wang, M.J. Zaworotko, 18-Fold Interpenetration and Concomitant Polymorphism in the 2:3 Co-Crystal of Trimesic Acid and 1,2-Bis(4-pyridyl)ethane, Cryst. Growth Des.**5** (2005) 2046-2049.

[8] M. Sarkar, K. Biradha, Amide-to-Amide Hydrogen Bonds in the Presence of a Pyridine Functionality: Crystal Structures of Bis(pyridinecarboxamido)alkanes, Cryst. Growth Des.**6** (2006) 202-208.

[9] A. Ballabh, D.R. Trivedi, P. Dastidar, Ascertaining the 1D Hydrogen-Bonded Network in Organic Ionic Solids, Cryst. Growth Des. **5** (2005) 1545-1553.

[10] M.N. Bhat, S.M. Dharma prakash, Growth of nonlinear optical γ-glycine crystals,J. Cryst. Growth 236 (2002) 376-380.

[11] C. Razzetti, M. Ardoino, L. Zaotti, M. Zha, C. Parorici, Solution Growth and Characterisation of L-alanine Single Crystals, Cryst.Res. Technol. **37** (2002) 456.

[12] C.B. Aakeroy, K.R. Seddon, The hydrogen bond and crystal engineering, Chem, Soc. Rev. **22** (1993) 397-407.

[13] M. Narayan Bhat, S. M. Dharma prakash, New nonlinear optical material: glycine sodium nitrate, J. Cryst. Growth, **235** (2002) 511-516.

[14] M. Narayan Bhat, S. M. Dharma prakash,Growth of nonlinear optical γ-glycine crystals, J. Cryst. Growth, **236** (2002), 376-80.

[15] P. Zaderenko, M. S. Gil, P. Lopez., P. Ballesteros, I. Fonseca, A. Albert, Diethyl 2-Benzimidazol-1-ylsuccinate-Picric Acid (1/1)-An Inclusion Molecular Complex, ActaCrystallogr. B, **53** (1997) 961-967.

[16] H. Basch, M. Krauss, W.J. Stevens, Cation binding effect on hydrogen bonding,J. Am. Chem. Soc. **107** (1985) 7267-7271.

[17] P.J. O’Malley,Hybrid Density Functional Studies of the Oxidation of Phenol-Imidazole Hydrogen-Bonded Complexes: A Model for Tyrosine Oxidation in Oxygenic Photosynthesis, J. Am. Chem. Soc. **120** (1998) 11732-11737.

[18] S. Scheiner, M. Yi, Proton Transfer Properties of Imidazole,J. Phys. Chem. **100** (1996) 9235-9241.

[19] W. Tatara, M.J. Wojcik, J. Lindgren, M. Probst, Theoretical Study of Structures, Energies, and Vibrational Spectra of the Imidazole−Imidazolium System, J. Phys. Chem. A **107** (2003) 7827-7831.

[20] C.C. Su, H.C. Chang, J.C. Jiang, P.Y. Wei, L.C. Lu, S.H. Lin,Evidence of charge-enhanced C–H–O interactions in aqueous protonated imidazole probed by high pressure infrared spectroscopy, J. Chem. Phys. **119** (2003)10753-10758.

[21] N.J. Kim, H. Kang, Y.D. Park, S.K. Kim, Dispersed fluorescence spectroscopy of jet-cooled adenine, Phys. Chem. Chem. Phys. **6** (2004) 2802.

[22] P. Dhamodharan, K. Sathya, M. Dhandapani, Studies on synthesis, structural, luminescent and thermal properties of a new non-linear optical crystal: 4-amino-4H-1,2,4-triazol-1-ium-3-hydroxy-2,4,6-trinitrophenolate, Physica B **508** (2017) 33-40.

[23] K. Sathya, P. Dhamodharan, M. Dhandapani, Computational, spectral and structural studies of a new non linear optical crystal: 2-hydroxy pyridinium 3,5-dinitrobenzoate,J. Mol. Struct.**1130** (2017) 414-424.

[24] P. Dhamodharan, K. Sathya, M. Dhandapani, Systematic evaluation of a new organic material:1-methyl-1H-imidazol-3-ium-2,4,6-trinitrobenzene-1,3-bis(olate)for

optoelectronics through spectral, structural, electrical, optical, quantum chemical and Hirshfeld surface studies, J. Phy. Chem. Solids, **104** (2017) 175-184.

[25] D.L. Pavia, G.M. Lampman and G.S. Kriz: Introduction to Spectroscopy, Washington, 2001, Page No. 36.

[26] A. Rathika, L. Guru Prasad and R. Ganapathi Raman: Physicochemical properties of Dimethylammonium-p-nitrophenolate-p-nitrophenol: A nonlinear Optical Crystal, Physica B**, 485** (2016) 29-34.

[27] D.K. Schroder: Semiconductor Material and Device Characterization, Wiley, New York, 1990.

[28] G. Blasse and B.C. Grabmaier: Luminescent Materials, Springer, New York, 1994.

[29] C.R. Ronda: Phosphors for lamps and displays: an applicational view, J. Alloys Compd., **225** (1995) 534-538.

[30] Y.W. Tan and C. S. Shi: Optical Spectroscopy Properties and Charge Compensation of $BaLiF_3$Doped with Ce^{3+}, J. Solids State Chem.,**150** (2000)178-182.

[31] B. W. Mott: Micro Indentation Hardness Testing, Butterworth, London, 1996

[32] N. Mansour, A. Momeni, R. Karimzadeh and M. Amini:Blue-green luminescent siliconnanocrystals fabricated by nanosecond pulsed laser ablation in dimethyl sulfoxide, Opt. Mater. Exp.,**2** (2012) 740.

[33] G.M. Sheldrick, SHELXS-97, A Program for Solution of Crystal Structures, University of Gottingen, Germany, 1997.

[34] G.M. Sheldrick, SHELXL-97, A Program for Solution of Crystal Structures, University of Gottingen, Germany, 1997.

[35] T. Yakhanthip, N. Kungwan, J. Jitonnom, P. Anuragudom, S.Jungsuttiwong and S. Hannongbua:Theoretical Investigation on the Electronic and Optical Properties of Poly(fluorenevinylene) Derivatives as Light-Emitting Materials, International Journal of Photo energy,**2011** 2011) 1-9.

[36] Y. Sheena Mary, C. YohannanPanicker, M. Sapnakumari, B. Narayana, B.K. Sarojini and Abdulaziz A. Al-Saadi: Molecular structure, FT-IR, vibrational assignments, HOMO-LUMO analysis and molecular docking study of 1-[5-(4Bromophenyl)-3-(4-fluorophenyl)-4,5-dihydro-1H-pyrazol-1-yl]ethanone, Spectrochim. Acta, Part A,**136** (2015) 473-482.

[37] C.M. Castro, M.C.R. Delgado, V. Hernandez, S. Hotta, J. Casoda and J.T.L. Navarrete:Efficiency of the p conjugation in a novel family of a, a'-bisphenyl end capped oligothiophenesby means of Raman spectroscopy,J. Chem. Phys., **116** (2002) 10419-10427.

[38] A.Najiya, C. YohannanPanicker, M. Sapnakumari, B. Narayana, B.K. Sarojiniand C. Van Alsenoy:Molecular structure, FT-IR, first orderhyperpolarizability, NBO analysis, HOMO and LUMO, MEP analysis of (E)-3- (4-chlorophenyl)-1-(4-fluorophenyl)prop-2-en-1-one by HF and density functional methods, Spectrochim. Acta, Part A,**133** (2014) 526-533.

[39] S. Karthigha, S. Kalainathan, Kunda Uma MaheswaraRao, Fumio Hamada, Manabu Yamada and Yoshihiko Kondo:Synthesis, growth, structural, optical, luminescence, surface and HOMO LUMO analysis of 2-[2-(4-cholro-phenyl) vinyl]-1-methylquinolinium naphthalene-2-sulfonate organic single crystals grown by a slow evaporation technique, J. Cryst. Growth,**436** (2016) 113-124.

[40] R.S. Mulliken: Electronic Population Analysis on LCAO-MO Molecular Wave Functions, *J. Chem. Phys.*,**23** (1955) 1833-1840.

[41] S.K. Wolff, D.J. Grimwood, J.J. McKinnon, D.Jayatilaka and M.A. Spackman: Crystal Explorer 3.1, University of Western Australia, Perth, Australia, 2007.

Table captions

Table 1 **Experimental and theoretical, ^{1}H and ^{13}C NMR of chemical shifts for IMHTP [δ ppm]**

Table 2. Comparison of experimental and calculated bond lengths (Å) and bond angles (°) of IMHTP

Table 3. Crystal data and structure refinement for IMHTP

Table 4. Comparison of first order hyperpolarizability for the constituents of IMHTP

Table 1 Experimental and theoretical, ^1H and ^{13}C NMR of chemical shifts for IMHTP [δ ppm]

Atom positions	Experimental	B3LYP/6-311g(d,p)			
		Gas	DMSO	Methanol	Water
H1	13.1	12.1240	12.1289	12.1283	12.1296
H2	7.7	8.9325	8.9849	8.9842	8.9856
NH	-	18.0692	17.2614	17.2714	17.2521
H3	9.1	8.9839	8.7591	8.7611	8.7573
NH	-	8.4845	9.3017	9.2904	9.3122
H6	8.6	6.9324	7.3237	7.3184	7.3286
H5	8.6	7.7967	7.5928	7.5965	7.5894
C3	156.2	159.5190	159.9056	159.8942	159.9163
C2	135.5	142.1514	142.2155	142.2118	142.2190
C1	156.2	168.8187	169.7316	169.7176	169.7448
C4	135.5	141.3290	142.1117	142.0960	142.1266
C5	126.1	131.7889	133.2855	133.2561	133.3132
C6	135.5	125.3815	126.9653	126.9316	126.9971
C7	134.8	141.1361	140.5094	140.5093	140.5098
C8	119.7	120.3899	124.3238	124.2698	124.3740
C9	119.7	127.6505	124.5675	124.6191	124.5191

Table 2. Comparison of experimental and calculated bond lengths (Å) and bond angles (°) of IMHTP

O(9)-C(3)	1.322	1.35	O(6)-N(3)-O(5)	121.9	123.2
N(3)-O(6)	1.204	1.266	O(6)-N(3)-C(6)	120.2	119.2
N(3)-O(5)	1.215	1.273	O(5)-N(3)-C(6)	117.9	117.5
N(3)-C(6)	1.452	1.453	C(5)-C(6)-C(1)	123	122.3
O(3)-N(2)	1.24	1.3	C(5)-C(6)-N(3)	117.1	117.3
C(6)-C(5)	1.358	1.372	C(1)-C(6)-N(3)	120	120.3
C(6)-C(1)	1.444	1.449	O(7)-C(1)-C(2)	120.8	123.1
O(4)-N(2)	1.219	1.264	O(7)-C(1)-C(6)	127.2	122
C(1)-O(7)	1.235	1.279	C(2)-C(1)-C(6)	112	114.6
C(1)-C(2)	1.429	1.444	C(6)-C(5)-C(4)	121.5	120.8
C(5)-C(4)	1.38	1.4	C(3)-C(2)-C(1)	126.9	123.6
C(2)-C(3)	1.367	1.397	C(3)-C(2)-N(1)	117.3	118.9
C(2)-N(1)	1.454	1.445	C(1)-C(2)-N(1)	115.7	117.4
N(1)-O(2)	1.211	1.258	O(2)-N(1)-O(1)	123.7	122.6
N(1)-O(1)	1.212	1.281	O(2)-N(1)-C(2)	117.7	120
N(2)-C(4)	1.411	1.424	O(1)-N(1)-C(2)	118.6	117.2
C(3)-C(4)	1.421	1.427	O(4)-N(2)-O(3)	120.6	121.2
C(8)-N(4)	1.296	1.387	O(4)-N(2)-C(4)	120.3	120
C(8)-C(9)	1.353	1.366	O(3)-N(2)-C(4)	119.1	118.6
C(7)-N(4)	1.317	1.332	O(9)-C(3)-C(2)	119.4	119.4
C(7)-N(5)	1.359	1.354	O(9)-C(3)-C(4)	124	122.5
C(9)-N(5)	1.332	1.396	C(2)-C(3)-C(4)	116.6	118
N(4)-C(7)-N(5)	107.5	107.4	C(5)-C(4)-N(2)	119.4	118.3
N(5)-C(9)-C(8)	107.3	106.1	C(5)-C(4)-C(3)	120	120.3
C(9)-N(5)-C(7)	107.2	109.3	N(2)-C(4)-C(3)	120.6	121.2
C(8)-N(4)-C(7)	109.6	109.7	N(4)-C(8)-C(9)	108.4	107.2
O(9)-C(3)	1.322(3)	1.35	O(6)-N(3)-O(5)	121.9(3)	123.2
RMSD values for Bond lengths and Bond angles are **0.017 Å and 1.556°,** respectively.					

*Calculated from optimized structure from DFT.

Table 3. Crystal data and structure refinement for IMHTP

Empirical formula	$C_9 H_7 N_5 O_8$	
Formula weight	313.20	
Temperature	293(2) K	
Wavelength	0.71073 Å	
Crystal system	Monoclinic	
Space group	$P2_1/c$	
Unit cell dimensions	a = 6.0000(12) Å	α= 90°.
	b = 13.100(3) Å	β= 94.00(3)°.
	c = 15.000(3) Å	γ = 90°.
Volume	1176.1(4) $Å^3$	
Z	4	
Density (calculated)	1.769 Mg/m^3	
Absorption coefficient	0.158 mm^{-1}	
F(000)	528	
Crystal size	0.18 x 0.15 x 0.12 mm^3	
Theta range for data collection	2.07 to 26.31°.	
Index ranges	-7<=h<=7, -16<=k<=16, -18<=l<=18	
Reflections collected	12093	
Independent reflections	2368 [R(int) = 0.0268]	
Completeness to theta = 26.31°	98.8 %	
Refinement method	Full-matrix least-squares on F^2	
Data / restraints / parameters	2368 / 0 / 200	
Goodness-of-fit on F^2	1.067	
Final R indices [I>2sigma (I)]	R1 = 0.0718, wR2 = 0.2266	
R indices (all data)	R1 = 0.0759, wR2 = 0.2322	
Largest diff. peak and hole	0.615 and -0.710 e.$Å^{-3}$	

Table 4. Comparison of first order hyperpolarizability for the constituents of IMHTP

Parameters	**b3lyp/6-311g**	**‘β’ tensor components**	**IMHTP**
μ_x	-15.081	xxx	-604.781
μ_y	-2.535	xxy	-53.293
μ_z	-2.366	xyy	-51.805
μ	**15.475**	yyy	-51.295
α_{xx}	-74.070	zxx	-38.224
α_{xy}	6.665	xyz	-11.863
α_{yy}	-148.651	zyy	-23.269
α_{xz}	11.54	xzz	5.239
α_{yz}	2.193	yzz	0.183
α_{zz}	-125.735	zzz	-0.767
α_0	116.1523	$\boldsymbol{\beta}_{\mathbf{total}}$	$\mathbf{5.724*10^{-30}}$ **esu**
α	$\mathbf{17.191*10^{-24}}$ **esu**		

Figure captions

Fig. 1. FT-IR and Raman spectra of IMHTP

Fig. 2. ^{1}H and ^{13}C NMR spectra of IMHTP

Fig. 3. (a) ORTEP plot (50% probability level) and (b) Optimized molecular structure of IMHTP

Fig. 4. Packing view and Hydrogen bonding network of IMHTP

Fig. 5. Frontier molecular orbitals of IMHTP

Fig. 6. Molecular electrostatic potential of IMHTP

Fig. 7. Mulliken charge distribution chart of IMHTP

Fig. 8. 2D fingerprint plots and its percentage contributions of IMHTP

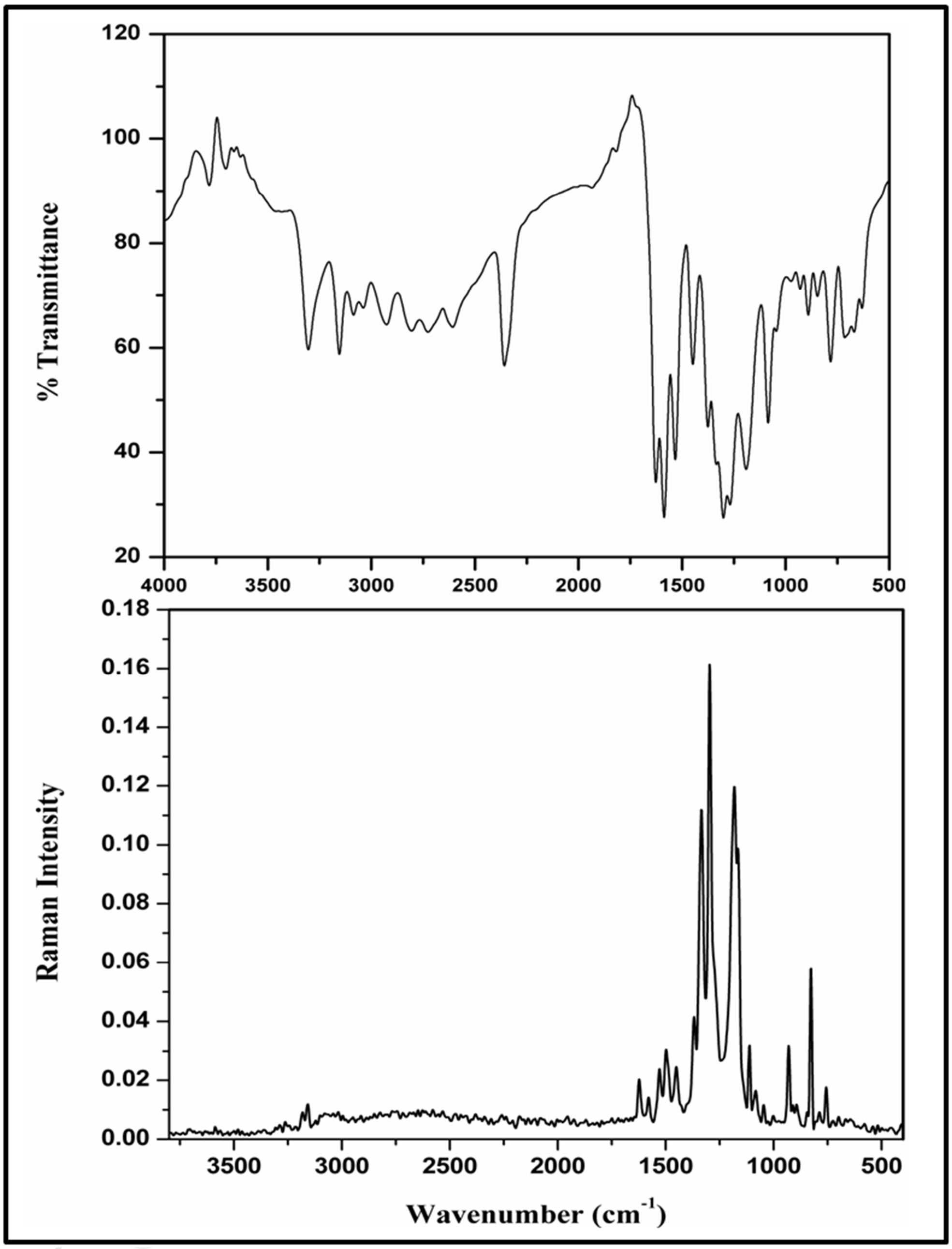

Fig. 1. FT-IR and Raman spectra of IMHTP

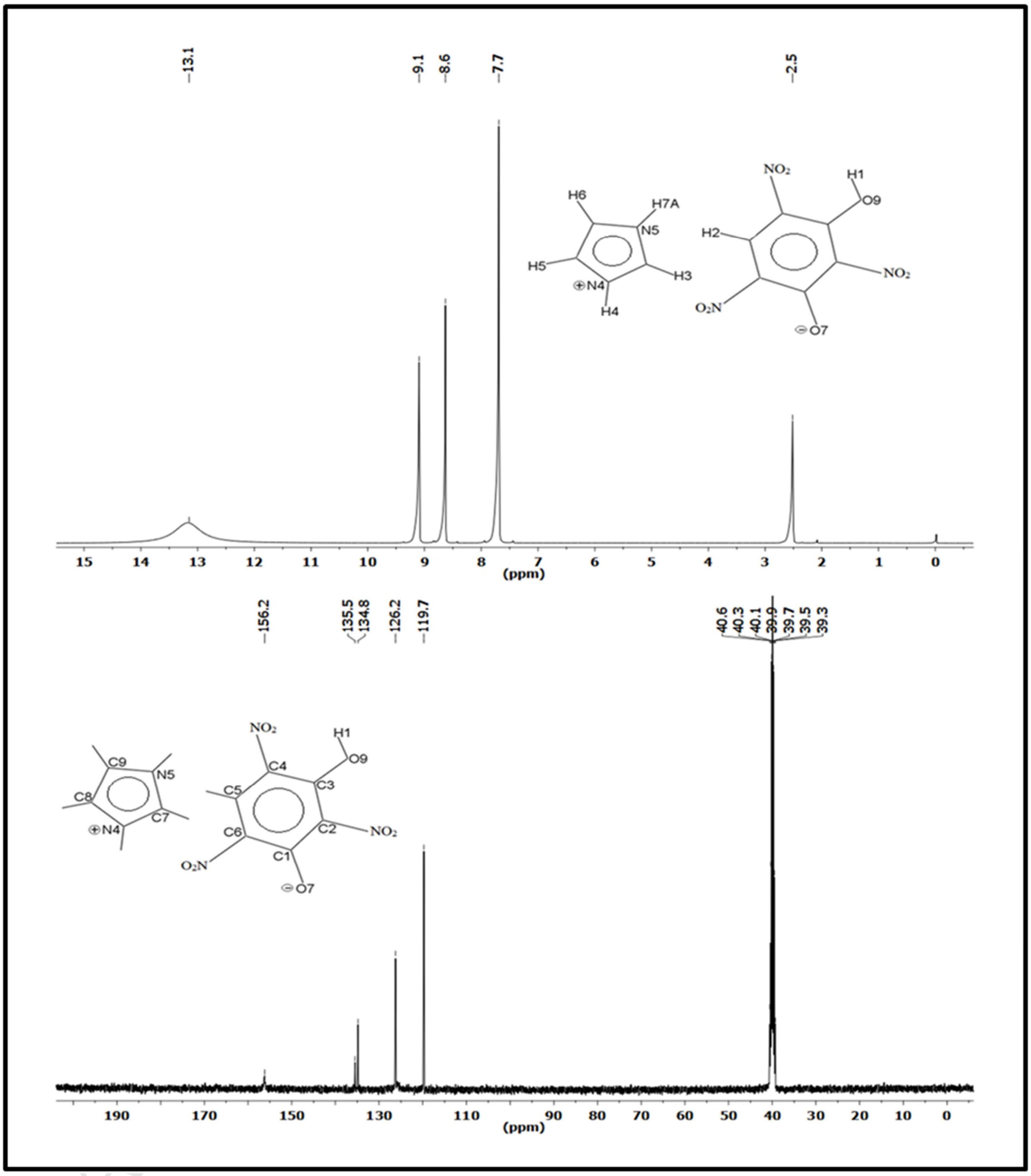

Fig. 2. ^{1}H and ^{13}C NMR spectra of IMHTP

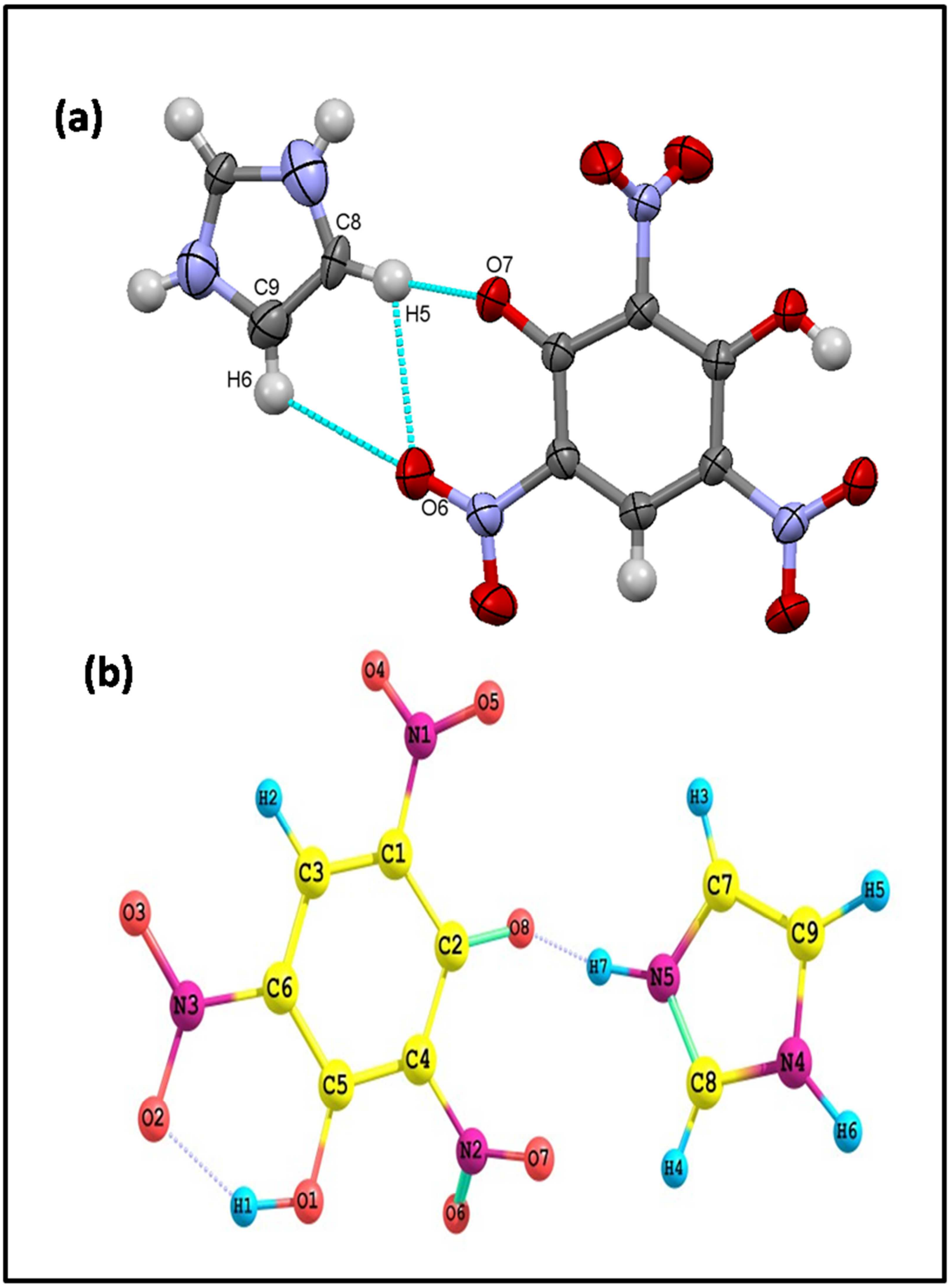

Fig. 3. (a) ORTEP plot (50% probability level) and (b) Optimized molecular structure of IMHTP

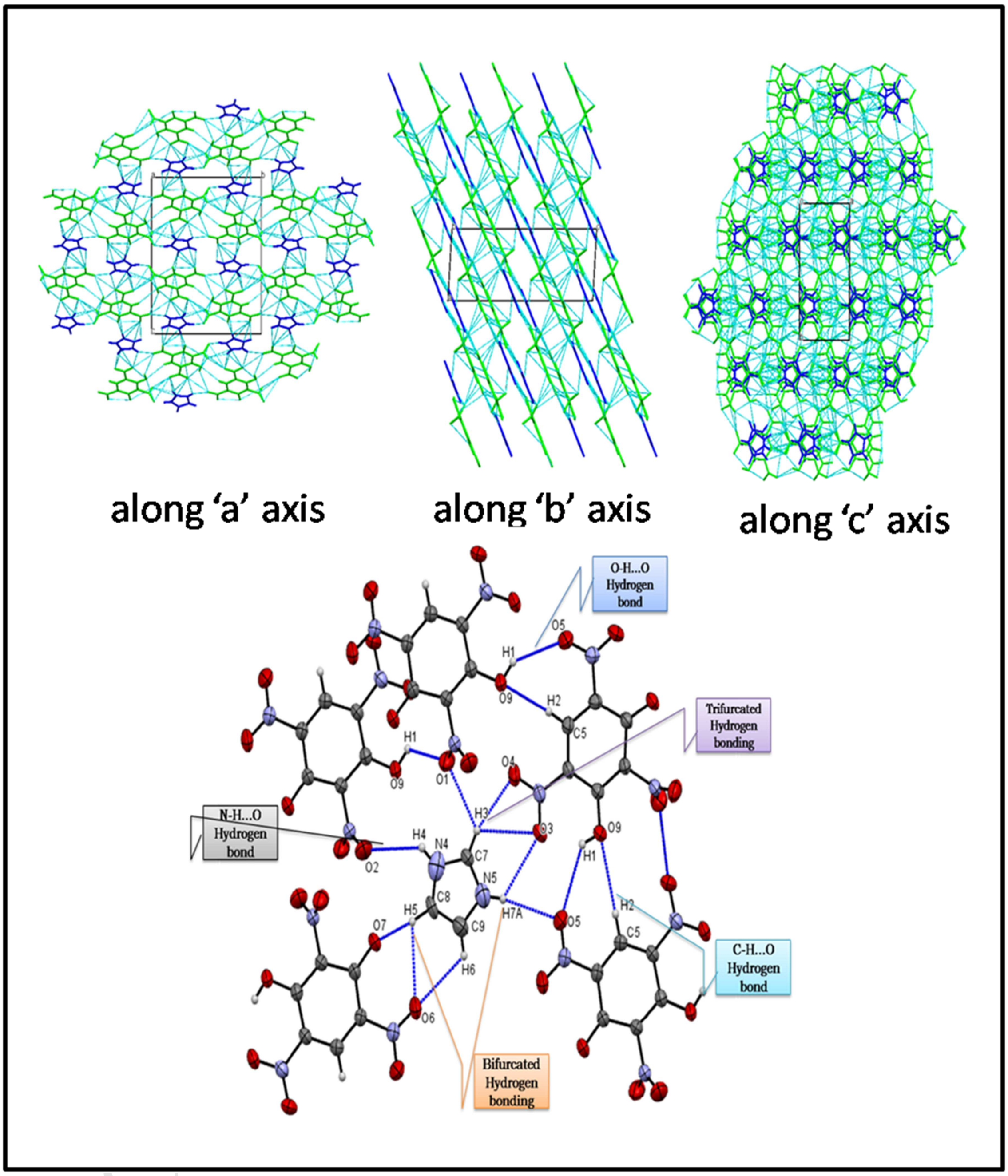

Fig. 4. Packing view and Hydrogen bonding network of IMHTP

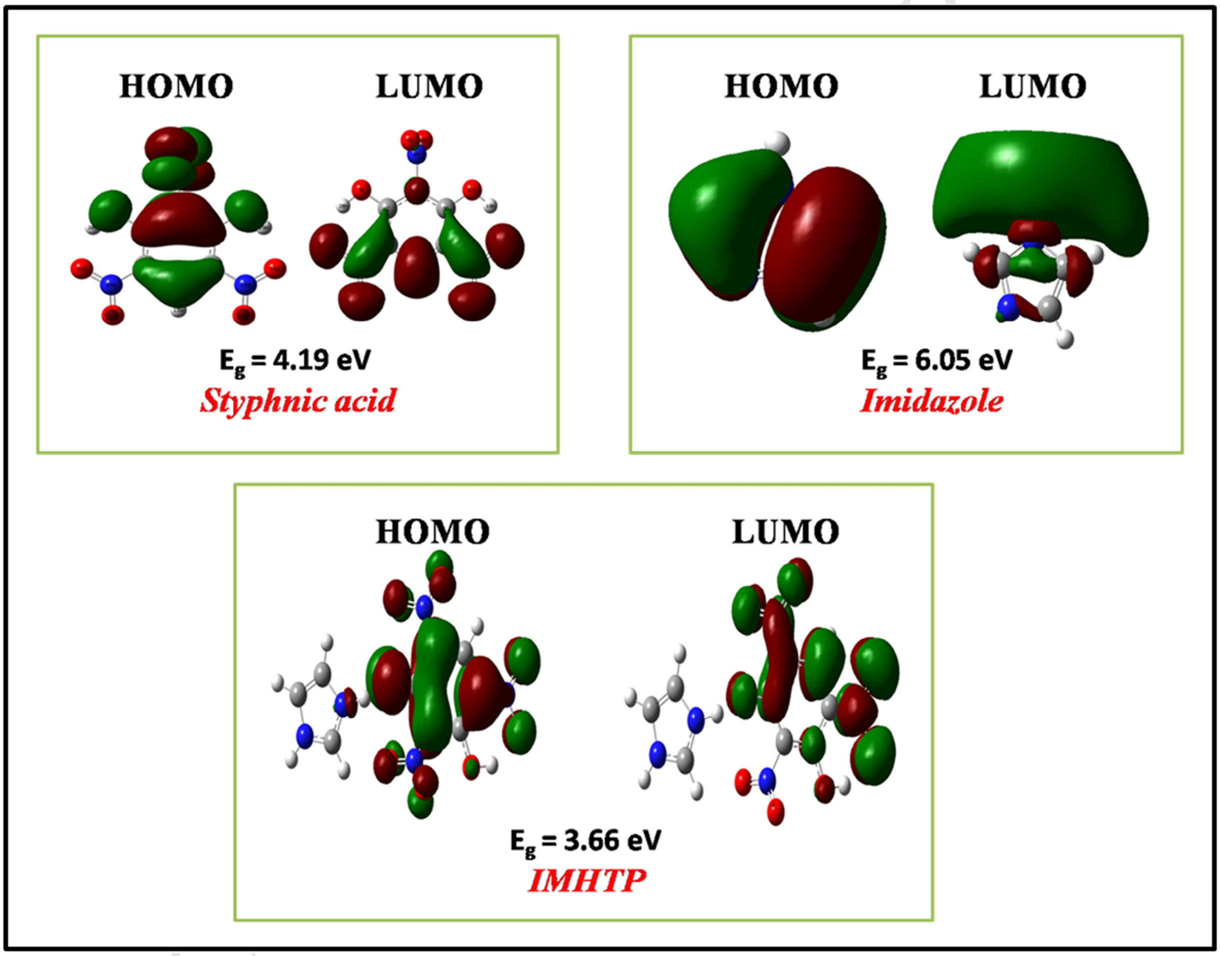

Fig. 5. Frontier molecular orbitals of IMHTP

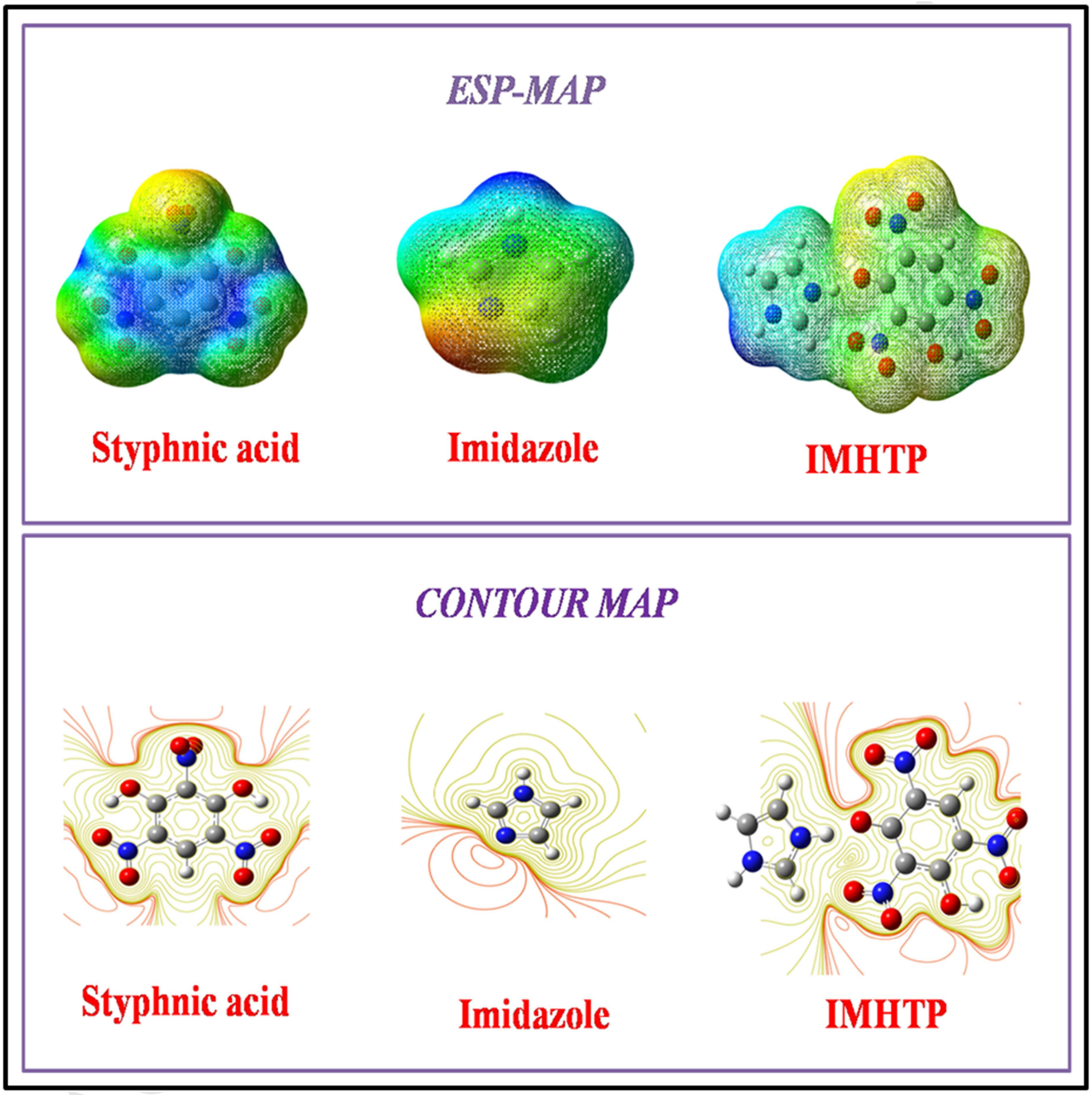

Fig. 6. Molecular electrostatic potential of IMHTP

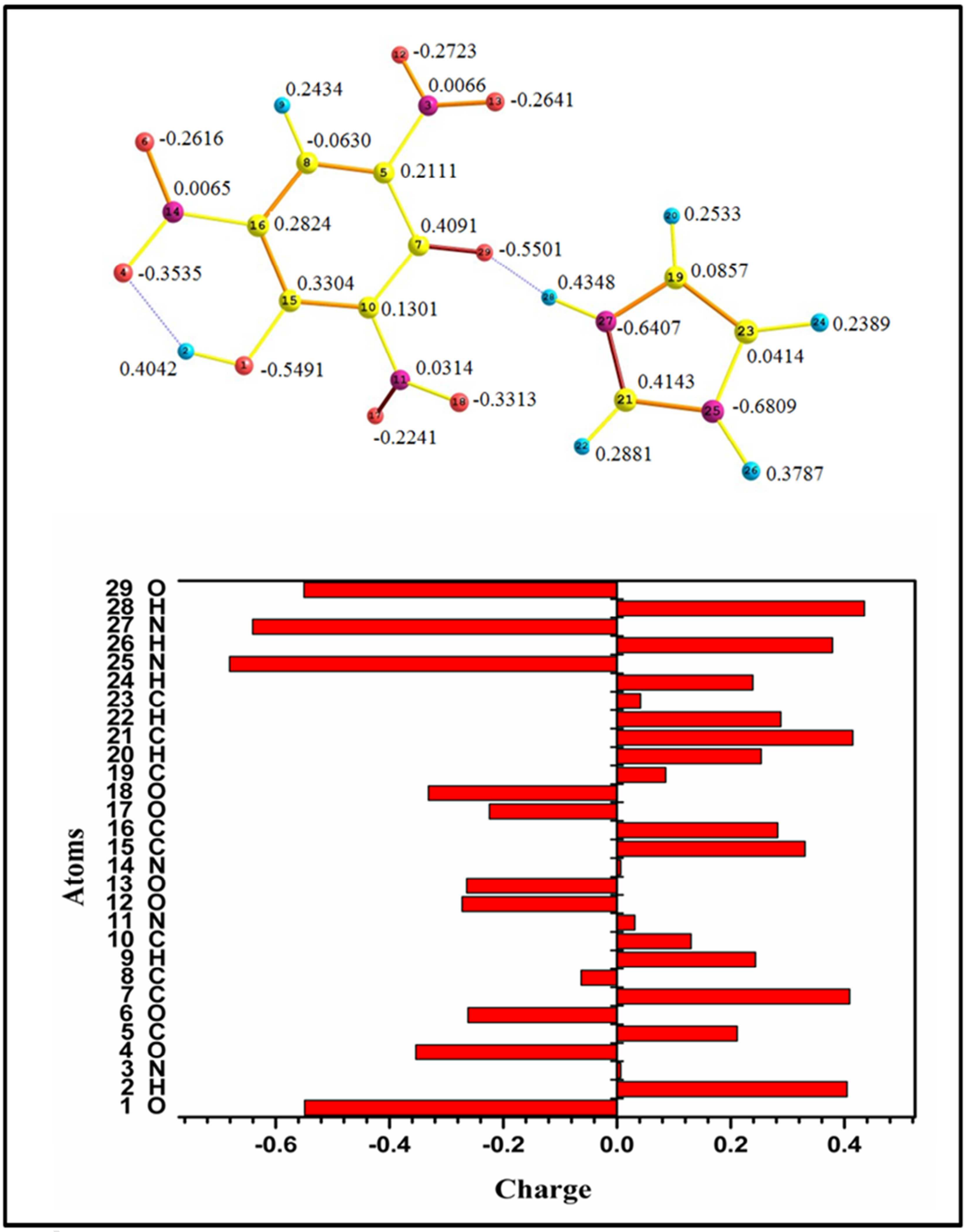

Fig. 7. Mulliken charge distribution chart of IMHTP

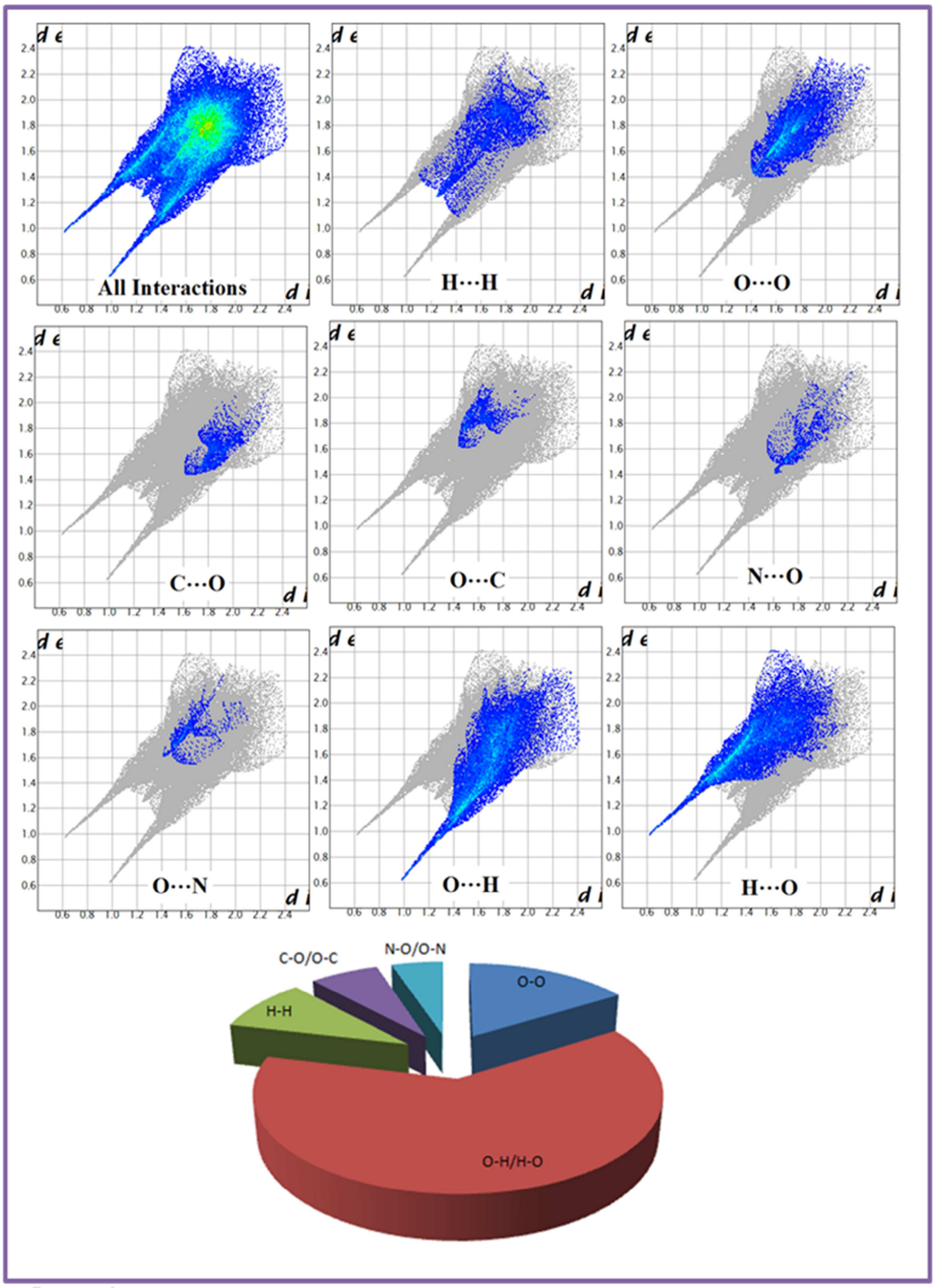

Fig. 8. 2D fingerprint plots and its percentage contributions of IMHTP

Highlights:

- IMHTP crystallizes in monoclinic system with space group $P2_1/c$
- The formation of the IMHTP was confirmed by NMR and FTIR
- IMHTP was found to be thermally stable up to 198 °C
- The first-order hyperpolarizability (β) of IMHTP is 5.724×10^{-30} esu.